Cooperative polymer dynamics under nanoscopic pore confinements probed by field-cycling NMR relaxometry

Nail Fatkullin
Department of Physics, Kazan State University, Kazan 420008, Tatarstan, Russia

Ravinath Kausik and Rainer Kimmich
Sektion Kernresonanzspektroskopie, Universität Ulm, 89069 Ulm, Germany

(Received 29 December 2006; accepted 18 January 2007; published online 6 March 2007)

Reptational dynamics of bulk polymer chains on a time scale between the Rouse mode relaxation time and the so-called disengagement time is not compatible with the basic thermodynamic law of fluctuations of the number of segments in a given volume. On the other hand, experimental field-cycling NMR relaxometry data of perfluoropolyether melts confined in Vycor, a porous silica glass of nominal pore dimension of 4 nm, closely display the predicted signatures for the molecular weight and frequency dependences of the spin-lattice relaxation time in this particular limit, namely $T_1 \propto M^{-1/2}\nu^{1/2}$. It is shown that this contradiction is an apparent one. In this paper a formalism is developed suggesting cooperative chain dynamics under nanoscopic pore confinements. The result is a cooperative reptational displacement phenomenon reducing the root-mean-squared displacement rate correspondingly but showing the same characteristic dependences as the ordinary reptation model. The tube diameter effective for cooperative reptation is estimated on this basis for the sample system under consideration and is found to be of the same order of magnitude as the nominal pore diameter of Vycor. © *2007 American Institute of Physics*. [DOI: 10.1063/1.2646367]

I. INTRODUCTION

The motivation to study polymer chain dynamics under mesoscopic confinements is twofold. Firstly, molecular motions and diffusion of molecules in porous media are of topical interest since many natural and technological materials actually have a porous nature. Even more important is, however, the second reason: The conditions under which polymer chains fluctuate under pore confinements are well defined and promise further elucidation of the fundamental laws governing macromolecular dynamics. In this sense, the key question of the present study refers to the degree of cooperativity of polymer chain motions.

In contrast to bulk polymer melts, there is a strong tendency of polymer melts confined in mesoscopic pores to show features predicted by the tube/reptation model both above and below the bulk critical molecular weight. In our previous papers,[1–4] this was demonstrated with confinements on a length scale from about 10 nm up to 1 μm using the field-cycling NMR relaxometry technique.[5] The spin-lattice relaxation time T_1 was measured as a function of the Larmor frequency ν and the weight-averaged molecular weight M_w. In a series of previous studies, the well-known limits of the ordinary tube/reptation model[6] have already been translated to predictions for the spin-lattice relaxation. The frequency and molecular weight dependences of T_1 thus are unambiguous and directly accessible indicators of these limits in extremely wide ranges. An overview of the spin-lattice relaxation laws suggested by the tube/reptation model and other polymer dynamics formalisms can be found in Ref. 7.

The prediction for limit II of the Doi/Edwards formalism for a time range between the so-called entanglement time τ_e and the Rouse relaxation time τ_R, namely, the characteristic law for the frequency and molecular weight dependences of the spin-lattice relaxation time $T_1 \propto M^0\nu^{3/4}$, was very well reproduced, whereas no such signatures were ever observed in bulk melts.[7–9] Remarkably, confinement phenomena of this tendency summarized as the so-called corset effect were found both above and below the bulk critical molecular weight[1] and even in micrometer thick polymer melt layers relative to bulk samples.[4]

However, the conclusion that the ordinary tube/reptation model[6] explains the dynamic behavior of polymer melts under mesoscopic confinements cannot be generalized to all limits predicted by this formalism. In Ref. 10, it was argued that specifically limit III, that is, the regime of reptation in the proper sense predicted for a time scale between τ_R and the so-called disengagement time τ_d, is not compatible with the restriction imposed on the fluctuations of the number of segments in a given volume by a fundamental law of statistical physics. Nevertheless, the molecular weight and frequency features of spin-lattice relaxation in limit III, that is, $T_1 \propto M^{-1/2}\nu^{1/2}$, were indeed closely approached in polymer melts confined to nanoscopic pores of a silica glass.[11]

The purpose of the present study is to show that the contradiction of these experimental findings to the incompatibility of limit III of the tube/reptation model with the thermodynamic principles is an apparent one. It will turn out that cooperativity of chain dynamics under nanoscopic confinements is the key to the understanding of this discrepancy.

II. EXPERIMENT

Fluorine 19 spin-lattice relaxation dispersion was studied with the aid of the field-cycling NMR relaxometry

technique.[5] A Stelar relaxometer covering frequencies in the range of 1 kHz to 40 MHz was employed. The field-cycling relaxometer is equipped with homemade auxiliary coils for the compensation of the earth field and stray fields from other magnets in the laboratory. The precision of the field cycles was checked with the aid of a fast Hall teslameter (Projekt Elektronik FM 210) probing the flux density at the sample position during test field cycles. The measuring bandwidth of the teslameter is 35 kHz, the resolution is 0.01 mT. Within the experimental error, all relaxation curves could be described by monoexponential functions over about one decade of the signal amplitude. In each experiment, all data have been measured twice by varying the frequency from high to low values and the other way round. The same values were found. Typical experimental errors were a few percent and never exceeded 5% under the most unfavorable conditions.

Vycor porous glass VPQ 7930 was purchased from Corning Ltd. It consists of 96% SiO_2. The nominal mean pore size is 4 nm (±0.6 nm) and the porosity is 28% according to specifications by the manufacturer. The specific surface area is 250 m^2/g, and the apparent density (dry) is 1500 kg/m^3. The samples were pretreated by boiling them for 60 min in 30% H_2O_2. After that, they were washed with distilled water and evacuated at 130 °C for 24 h. The samples were then considered to be dry and empty.

In order to test the influence of any polymer/surface adsorption effect, the Vycor samples were modified by nonpolar surface coating.[12] This was carried out by first washing the glass with petroleum ether and then dipping them in a solution of trimethyl siloxy groups. After a period of about 30 min the porous glass was removed and then washed with petroleum ether again. This process is expected to result in evenly surface coated porous glass. However, the effect of silanization on the spin-lattice relaxation dispersion of polymers filled into the pore space was found to be remarkably small. Data for samples without surface coating can be found in Ref. 11.

The polymer used is a perfluoropolyether [PFPE; Krytox; $(F(-CF(CF_3)-CF_2-O-)_nCF_2-CF_3)$] and all measurements correspond to fluorine spin-lattice relaxation dispersion curves. The polymer was evacuated at 130 °C in vacuum of 10 mbars for about 24 h to take out all traces of residual moisture. The polymers were then filled into the porous glass with the aid of the bulk-to-bulk method. To get completely filled pores the process was carried out for a period of 2 weeks. All experiments were performed at least 5 h after taking out the filled porous glass so that equilibrium is attained. The experiments were also repeated after a period of 4 weeks to test the stability of the system.

III. THEORY OF COOPERATIVE CHAIN DYNAMICS IN MESOSCOPIC PORES

Consider a polymer melt confined in an infinite cylindrical pore of mesoscopic diameter $d_{\text{pore}}=2R$ and radius R (see Fig. 1). Let the number of Kuhn segments per chain be N_{chain} and the Kuhn segment length b. The macromolecules consequently have an extended conformation considered to be composed of blobs of characteristic length d_{pore}. On the average, each blob contains about d_{pore}^2/b^2 Kuhn segments. A polymer chain of length $L=N_{\text{chain}}b$ will therefore be extended along the pore axis a distance

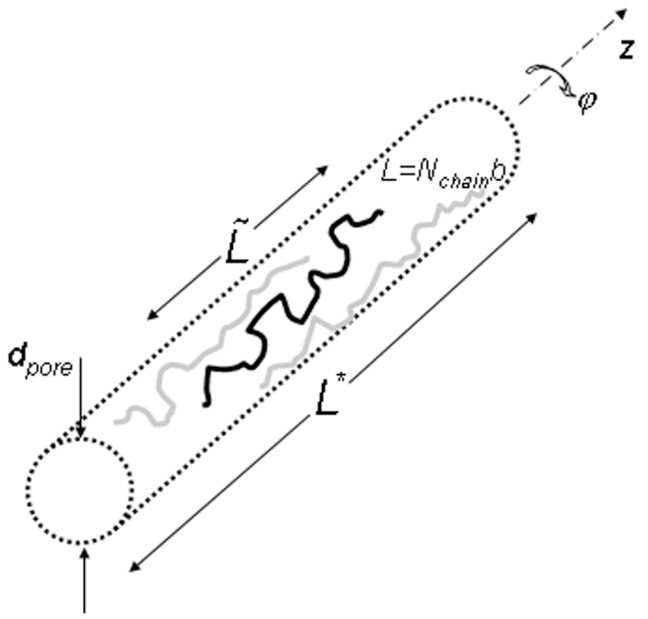

FIG. 1. Schematic representation of the cyclindrical model pore on which the formalism is based. The "tagged" chain (black) moves cooperatively with neighboring chains (gray) in the pore.

$$\tilde{L} \approx d_{\text{pore}} N_{\text{chain}} b^2/d_{\text{pore}}^2 = Lb/d_{\text{pore}}. \tag{1}$$

A section of length $\tilde{L}$ of the cylindrical pore has a volume of the order of $d_{\text{pore}}^2\tilde{L}$ and contains

$$\langle N_V \rangle \cong \rho_s d_{\text{pore}}^2 \tilde{L} = \rho_s b^2 d_{\text{pore}} N_{\text{chain}} = N_{\text{chain}} d_{\text{pore}}/p \tag{2}$$

Kuhn segments on the average, where ρ_s is the number density of Kuhn segments and $p=1/\rho_s b^2$ is the so-called packing length.

A. Cooperative rotational diffusion modes

Provided that the pore diameter d_{pore} is not too large, rotational diffusion of the polymer chains around the pore axis can contribute significantly to the dynamics in the time limit $t \ll \tau_t \propto \tau_s N_{\text{chain}}^3$, where τ_t is the terminal chain mode relaxation time and τ_s is the segment fluctuation time. Let the length of the confining pore be $L^* \gg \tilde{L} \gg d_{\text{pore}}$. The orientation is assumed along the z axis. Under these conditions, the polymer melt reacts to torsions like an elastic solid. That is, it can be treated as a thin solid rod being subjected to torsional modes with friction at the pore surfaces.

Let $\varphi(z,t)$ be the torsion angle of the polymer melt around the pore axis at position z and time t (see Fig. 1). For nonvanishing gradient, $(\partial/\partial z)\varphi(z,t) \neq 0$, the elasticity of the polymer melt tends to restore the deformation by the restitutive stress it produces. The equation of motion of a cross-sectional slice of thickness unity of a circular rod reads (compare, for example, Ref. 13)

$$I\frac{\partial^2}{\partial t^2}\varphi(z,t) + \zeta_{\mathrm{rot}}\frac{\partial}{\partial t}\varphi(z,t) = C\frac{\partial^2}{\partial z^2}\varphi(z,t) + F^L(z,t), \tag{3}$$

where

$$I = \rho_m\frac{\pi}{2}R^4 \tag{4}$$

is the moment of inertia per unit length about the long axis, $\rho_m = m_s\rho_s$ is the mass density of the polymer melt, m_s is the mass of a Kuhn segment, $C = G(\pi/2)R^4$ is the torsional spring constant per unit length, G is the shear modulus, and ζ_{rot} is the rotational friction coefficient per unit length between the polymer melt cylinder and the pore surface. The force $F^L(z,t)$ is the stochastic Langevin term arising from interactions with the surface. Note that Eq. (3) differs from the ordinary equation for rotational modes in the theory of elastic solids by a frictional and a Langevin term connected with it.

The second term on the left-hand side of Eq. (3) is the torque per unit length, T_f, acting on the polymer melt cylinder due to friction at the pore surface. Its magnitude obeys

$$T_f = \zeta_{\mathrm{rot}}\frac{\partial\varphi}{\partial t} = F_f R = \zeta_{\mathrm{trans}} v R, \tag{5}$$

where F_f is the friction force per unit length, $v = R\partial\varphi/\partial t$ is the tangential velocity at the cylinder surface, and ζ_{trans} is the ordinary friction coefficient of the polymer cylinder per unit length. From Eq. (5), we obtain the relation $\zeta_{\mathrm{rot}} = \zeta_{\mathrm{trans}}R^2$ between the rotational and ordinary friction coefficients. The number of Kuhn segments in a surface layer of thickness b per unit length of a polymer cylinder is

$$n_s = \frac{2\pi R}{b^2}\rho_s b^3 = 2\pi R\rho_s b. \tag{6}$$

Introducing the segmental friction coefficient ζ_s thus leads to the following expression for the rotational friction coefficient per unit length in terms of the segmental friction coefficient:

$$\zeta_{\mathrm{rot}} = n_s R^2\zeta_s = 2\pi R^3 b\rho_s\zeta_s = \frac{2\pi R^3}{bp}\zeta_s. \tag{7}$$

The characteristic time constant intrinsic to wave equations like Eq. (3) is given by the quotient of the coefficients of the inertia and friction terms. That is,

$$\tau_0 = \frac{I}{\zeta_{\mathrm{rot}}} = \frac{\rho_m(\pi/2)R^4}{2\pi R^3 b\rho_s\zeta_s} = \frac{m_s R}{4b\zeta_s} = \frac{1}{4}\frac{R}{b}\tilde{\tau}_0, \tag{8}$$

where we have made use of Eqs. (4) and (7) and the definition

$$\tilde{\tau}_0 \equiv \frac{m_s}{\zeta_s}. \tag{9}$$

In the short-time limit, $t \ll \tau_0$, the inertia term exceeds the friction term in Eq. (3), and torsional motions of the polymer melt cylinder around the z axis adopt the character of rotational oscillations about the initial orientation. In the opposite limit, $t \gg \tau_0$, the friction term dominates, and the torsions take up a diffusive character. The time constant $\tilde{\tau}_0$ defined in Eq. (9) typically is of the order $\tilde{\tau}_0 \simeq 10^{-13}$–$10^{-12}$ s in condensed matter which corresponds to a few atomic collisions. The typical values of the Kuhn segment length are in the range $b = 0.5$–1 nm. That is, the characteristic time obeys $\tau_0 < 10^{-9}$ s even for pores with relatively large diameters, $d_{\mathrm{pore}} \to 10^3$ nm. The inertia term can therefore safely be neglected, and Eq. (3) can be rewritten as

$$\zeta_{\mathrm{rot}}\frac{\partial}{\partial t}\varphi(z,t) \approx C\frac{\partial^2}{\partial z^2}\varphi(z,t) + F^L(z,t). \tag{10}$$

Here we see the main difference to the theory of rotation modes of solid rods: In the elasticity formalism, the inertia term dominates so that the time dependence of normal modes has a vibrational character. In the present case, the friction term is much larger, and normal modes of the relaxation type result from Eq. (10).

The time scale of interest is $t \ll \tau_s N_{\mathrm{chain}}^3$, which is much shorter than the terminal relaxation time suggested by Eq. (10), because we are considering the limit $L = N_{\mathrm{chain}}b \ll \tilde{L}$. That is, the influence of boundary conditions on the solutions of Eq. (10) is negligible in this case. As the simplest boundary condition we may therefore use

$$\left.\frac{\partial}{\partial z}\varphi(z,t)\right|_{z=0,\tilde{L}} = 0. \tag{11}$$

Under such conditions, Eq. (10) is analytically equivalent to the Rouse equation of motion for a chain with formally $\tilde{L}$ Kuhn segments, a segmental friction coefficient identified with ζ_{rot}, and a Kuhn segment length equivalent to $\tilde{b}$ defined by[6,7] $3k_BT/\tilde{b}^2 = C$. The ordinary Rouse equation reads

$$\zeta_s\frac{\partial}{\partial t}\mathbf{r}_n = \frac{3k_BT}{\tilde{b}^2}\frac{\partial^2}{\partial n^2}\mathbf{r}_n + F_n^L(t), \tag{12}$$

with the initial condition $(\partial/\partial n)\mathbf{r}_n|_{n=0,N} = 0$ and the segment numbers $0 \le n \le N$. In the limit $t \ll \tau_s N^2$, where $\tau_s = b^2\zeta_s/3\pi^2 k_BT$, the mean-squared displacement can be calculated as

$$\langle r^2(t)\rangle = \frac{2}{\pi^{3/2}}\tilde{b}^2\left(\frac{t}{\tau_s}\right)^{1/2}. \tag{13}$$

Taking into account the one-dimensional character of the variable $\varphi(z,t)$ in Eq. (10), we find analogously

$$\langle[\varphi(z,t) - \varphi(z,0)]^2\rangle = \frac{1}{3}\frac{2}{\pi^{3/2}}\tilde{b}^2\left(\frac{t}{\tau_s}\right)^{1/2} = \sqrt{\frac{4}{3\pi}\tilde{b}^2\frac{k_BT}{\zeta_{\mathrm{rot}}}t} = \sqrt{\frac{t}{\tau_{\mathrm{rot}}}}, \tag{14}$$

where

$$\tau_{\mathrm{rot}} = \frac{3\pi}{4}\frac{\tilde{b}^2\zeta_{\mathrm{rot}}}{k_BT} = \frac{\pi}{4}\frac{C\zeta_{\mathrm{rot}}}{(k_BT)^2} = \frac{\pi^3}{4}\frac{\mu\zeta_{\mathrm{trans}}R^7}{(k_BT)^2bp}. \tag{15}$$

In the limit $t \ll \tau_{\mathrm{rot}}$, the influence of rotational modes on segment dynamics is negligible but could be essential for $t \gg \tau_{\mathrm{rot}}$. However, the dependence of τ_{rot} on the pore radius is rather strong so that rotational modes in pores of sufficiently large size will not be relevant. To estimate a characteristic

pore size in this sense, the shear modulus μ is needed. As a reasonable approach, one can equate μ with the plateau modulus of the polymer melt,[6]

$$\mu = G_N^0 \simeq \frac{k_B T}{N_e}\rho_s, \tag{16}$$

where N_e is a phenomenological parameter often illustrated as the number of Kuhn segments between two neighboring so-called entanglements. An empirical value is $N_e \approx 25-50$ for most flexible polymers. Inserting Eq. (16) in Eq. (15) gives

$$\tau_{\mathrm{rot}} = \frac{\pi^3}{4N_e}\frac{\zeta_{\mathrm{trans}}R^7}{k_B T b^3 p^2} = \frac{\pi^3}{4N_e}\frac{\zeta_{\mathrm{trans}}b^2}{k_B T}\frac{R^7}{b^5 p^2} = \frac{\pi^3}{4N_e}\tau_{\mathrm{suf}}\frac{R^7}{b^5 p^2}, \tag{17}$$

with the definition

$$\tau_{\mathrm{suf}} = \frac{\zeta_{\mathrm{trans}}b^2}{k_B T}. \tag{18}$$

The quantity τ_{suf} has the dimension of time. It depends on interactions between polymer segments and the pore surface as represented by the friction coefficient ζ_{trans}, so that it can be considered as the segmental relaxation time at the pore surface.

The experimental time probed in NMR spin-lattice relaxation studies is $t_{\mathrm{expt}} \simeq 1/2\pi\nu$, where ν is the resonance frequency. Equating $\tau_{\mathrm{rot}} = t_{\mathrm{expt}}$ permits one to estimate a characteristic pore radius from Eq. (17):

$$\tilde{R} \simeq \left[\frac{4N_e}{\pi^3}\frac{t_{\mathrm{expt}}}{\tau_{\mathrm{suf}}}b^5 p^2\right]^{1/7} \simeq \left[\frac{t_{\mathrm{expt}}}{\tau_{\mathrm{suf}}}\right]^{1/7} b. \tag{19}$$

Assuming typical values $t_{\mathrm{expt}} \approx 10^{-7}$ s, $\tau_{\mathrm{suf}} \approx 10^{-11}$ s, and $b = 0.5-1$ nm suggests $\tilde{R} \simeq 4b \approx 5$ nm. That is, the rotational diffusion modes described above become experimentally relevant at frequencies below about 1 MHz.

In our previous work,[1,2] rotational diffusion modes of the polymer melt rod around the pore axis (see Fig. 1) were neglected. The argument was that very long chains confined in a cylindrical pore are expected to reptate inside their own tight tubes of diameter $d_{\mathrm{tube}} \simeq \sqrt{\rho_s b^2 \kappa_T k_B T}$, where κ_T is the isothermal compressibility of the polymer melt. The above consideration makes it clear that this conclusion is valid only for pores with diameters $d_{\mathrm{pore}} \gg 2\tilde{R}$, so that rotational modes are irrelevant. Actually all samples examined in Refs. 1 and 2 satisfied this condition in contrast to the present investigation referring to hundred times smaller pores. The situation examined in the present study is characterized by $d_{\mathrm{pore}} < 2\tilde{R}$. In this case, the effective tube diameter corresponds to the pore diameter, $d_{\mathrm{eff}} \hat{=} d_{\mathrm{pore}}$, and rotational modes are fully effective in the limit $t \gg \tau_{\mathrm{rot}}$.

B. Cooperative reptation of polymer chains confined in mesoscopic pores on a time scale longer than the Rouse relaxation time

Another very important issue which must be examined in this context is connected with thermodynamic limitations ordinary reptation may be subjected to. The mean-squared fluctuation of the number of segments in a given volume element depends on the isothermal compressibility according to a well-known, standard relation of statistical physics. It can be shown[10] that the tube/reptation model predicts fluctuations in bulk polymer melts larger than permitted by thermodynamics on a time scale $t \geqslant \tau_R$. That is, the reptation process cannot take place in bulk melts in the form literally anticipated by this particular model.[6] In the present treatment, polymer melts confined in mesoscopic cylindrical pores are considered. So bulk conditions do not apply. Therefore, things must be reassessed. In this context it should be made clear that the Rouse relaxation time τ_R in bulk and under confinement is not necessarily the same due to the different natures of the constraints.

The average number of Kuhn segments in a volume $V = \tilde{L}d_{\mathrm{pore}}^2$ is estimated to be of the order $\langle N_V \rangle = \rho_s V \simeq N_{\mathrm{chain}} d_{\mathrm{pore}}/p$ [see Eqs. (1) and (2)]. The number of tubes, n_t, having one end inside the considered volume V and the other outside is equal to the number of polymer chains with this property and can be estimated by

$$n_t \simeq \frac{\langle N_V \rangle}{N_{\mathrm{chain}}} = \frac{d_{\mathrm{pore}}}{p}. \tag{20}$$

According to the conventional tube/reptation model,[6] a polymer chain starts to reptate inside its own tube in the time limit $t \gg \tau_e = \tau_s (d_{\mathrm{tube}}/b)^4$, where τ_e is the so-called entanglement time after which segments sense the tube constraint and $\tau_s = \zeta_s b^2/(3\pi^2 k_B T)$ is the segmental relaxation time. The Rouse relaxation time is given by $\tau_R = \tau_s N_{\mathrm{chain}}^2$. Let us for the moment focus on the limit $t \gg \tau_R$, for which the reptation model predicts that polymer chains are coherently displaced curvilinear distances $s(t)$ along their tubes.

Thermal fluctuations of polymer chains in tubes are strongly restricted. The number of segments, $n(t)$, leaving their old tubes in an interval t is of the order of the number of segments contained in a tube section of curvilinear length $s(t)$. That is,

$$\frac{n(t)b^2}{d_{\mathrm{tube}}^2} = \frac{s(t)}{d_{\mathrm{tube}}} \text{ or } n(t) = \frac{s(t)}{b^2}d_{\mathrm{tube}}. \tag{21}$$

Reptation of polymer chains causes fluctuations of the number of segments in the considered volume $V \simeq \tilde{L}d_{\mathrm{pore}}^2$. According to the model, motions of chains inside their own tubes are independent of each other. The mean-squared fluctuation of segment number in V after a time t can therefore be estimated as

$$\langle [\delta N_V(t)]^2 \rangle_{\mathrm{rep}} \simeq n_t \langle n^2(t) \rangle, \tag{22}$$

where the angular brackets indicate an average over all stochastic processes connected with reptation of the chains. Combining Eqs. (20)–(22) leads to

$$\langle [\delta N_V(t)]^2 \rangle_{\mathrm{rep}} \simeq \frac{d_{\mathrm{pore}}}{p}\frac{\langle s^2(t) \rangle d_{\mathrm{tube}}^2}{b^4}. \tag{23}$$

On the other hand, the total mean-squared fluctuation of segments in a volume V obeys the known thermodynamic relation (see, for example, Ref. 14)

$$\langle(\delta N_V)^2\rangle = k_B T \rho_s \kappa_T \langle N_V\rangle. \tag{24}$$

From this, the inequality

$$\langle[\delta N_V(t)]^2\rangle_{\text{rep}} \leqslant \langle[\delta N_V]^2\rangle \tag{25}$$

follows. The left-hand side depends on time [see Eq. (23)] while the right-hand side does not. Based on Eqs. (2) and (23)–(25), this stipulates that the mean-squared curvilinear segment displacement is limited according to the inequality

$$\langle s^2(t)\rangle \leqslant \rho_s k_B T \kappa_T b^4 N_{\text{chain}} d_{\text{pore}}^{-2}. \tag{26}$$

The tube length is of the order

$$L_t \simeq b^2 N_{\text{chain}} d_{\text{pore}}^{-1}. \tag{27}$$

Equations (26) and (27) suggest that the thermodynamically permitted mean-squared displacements by reptation along the tubes are much shorter than the tube length:

$$\langle s^2(t)\rangle^{1/2} \leqslant (\rho_s k_B T \kappa_T b^4 N_{\text{chain}} d_{\text{pore}}^{-2})^{1/2} \ll L_t \simeq b^2 N_{\text{chain}} d_{\text{pore}}^{-1}. \tag{28}$$

The conclusion is that, solely based on standard reptation modes, polymer chains cannot diffuse over distances comparable to their linear size. In other words, reptation motions would cause fluctuations much larger than thermodynamically permitted in times long enough.

To express inequality (28) in terms of time scale limitations of the compatibility of the tube/reptation model with thermodynamics, it is necessary to use explicit expressions for the mean-squared displacement $\langle s^2(t)\rangle$ along the tube. In the limit $\tau_e \ll t \ll \tau_R$ (regime II), the mean-squared curvilinear displacement varies with time as

$$\langle s^2(t)\rangle \simeq \frac{2}{3\pi^{3/2}} b^2 \left(\frac{t}{\tau_s}\right)^{1/2}. \tag{29}$$

Inserting Eq. (28) leads to

$$t \leqslant \frac{9\pi^3}{4}\left[\frac{\rho_s k_B T \kappa_T b^2}{d_{\text{pore}}^2}\right]^2 \tau_R \propto \tau_R. \tag{30}$$

Limit III is defined by $\tau_R \ll t \ll \tau_t = 3\tau_s N_{\text{chain}}^3 (b^2/d_{\text{pore}}^2)$, where τ_t is the terminal relaxation time predicted by the reptation model. In this regime, the mean-squared curvilinear displacement obeys

$$\langle s^2(t)\rangle \simeq \frac{2}{3\pi^2} b^2 \frac{t}{N_{\text{chain}}\tau_s}. \tag{31}$$

Inserting inequality (28) again suggests the following restriction:

$$t \leqslant \frac{3\pi^2}{2} \rho_s k_B T \kappa_T \tau_R \frac{b^2}{d_{\text{pore}}^2} \propto \tau_R. \tag{32}$$

We conclude that the general thermodynamic relation [Eq. (24)] in principle allows ordinary reptation for times shorter than the Rouse relaxation time but makes it impossible for much longer times. The ordinary reptation model postulates that polymer chains move strictly independently of each other in their own tubes as reflected by the mathematical structure of Eq. (22). The consequence is that fluctuations along the pore axis on a length scale $\tilde{L} = Lb/d_{\text{pore}}$ are predicted for the limit $t \gg \tau_R$, which are much larger than thermodynamically allowed.

On the other hand, the tube restriction permits no other motion than reptation for polymer chains long enough so that the limit $\tilde{L} \gg d_{\text{pore}}$ applies. Therefore, the character of reptation motions should drastically change when reaching the limit $t \gg \tau_R$: It must be strongly cooperative in the sense that neighboring chains in different tubes move in a correlated manner by tendency. A good deal of the reptational modes considered in the ordinary reptation picture is expected to be frozen in, and the mean-squared curvilinear displacement given by Eq. (31) will be substantially reduced.

C. Spin-lattice relaxation in nanoscopic pores and the tube diameter effective for cooperative reptation

The prediction for the Rouse model in the Larmor angular frequency range $\tau_R^{-1} \ll \omega \ll \tau_s^{-1}$ is[7,15–17]

$$\frac{1}{T_1^{\text{Rouse}}} \approx 0.63\tau_s\left(\tilde{M}_2 \ln\left(\frac{0.95}{\omega\tau_s}\right) + \tilde{M}_2^*\right), \tag{33}$$

where $\tilde{M}_2$ is the residual second moment of spin interactions after averaging over all fast motions occurring on a time scale $t \ll \tau_s$ and $\tilde{M}_2^*$ is the total second moment of the unaveraged dipolar interactions. In Refs. 1 and 2, it was shown that the ordinary reptation model holds in the frame of the so-called corset effect. In the limit $\tau_R^{-1} \ll \omega \ll \tau_e^{-1}$ (Doi/Edwards limit II) one expects for polymer melts confined in mesoscopic pores

$$\frac{1}{T_1^{\text{rep,II}}} \approx \frac{32\pi^{1/4}3^{1/2}}{1215}\Gamma(5/4)\cos(\pi/8)(1+2(2^{1/4})) \times \frac{b^3\tilde{l}}{d_{\text{pore}}^4}\frac{\tilde{M}_2\tau_s}{(\omega\tau_s)^{3/4}}. \tag{34}$$

Likewise one finds for the limit $\tau_d^{-1} \ll \omega \ll \tau_R^{-1}$ (Doi/Edwards limit III)[11]

$$\frac{1}{T_1^{\text{rep,III}}} \approx \frac{32\pi^{1/2}3^{1/2}}{1215}\Gamma(1/2)\cos(\pi/4)(1+2^{3/2}) \times N_{\text{chain}}^{1/2}\frac{b^3\tilde{l}}{d_{\text{pore}}^4}\frac{\tilde{M}_2\tau_s}{(\omega\tau_s)^{1/2}}, \tag{35}$$

where τ_d is the so-called disengagement time.[6] Equation (34) was derived in Ref. 15 assuming confining tubes with harmonic radial potential. The quantity $\tilde{l}$ is the persistence length of the randomly coiled tube. Equation (35) was obtained analogously.

In the light of the conclusions of the previous section, Eq. (35) for limit III must be modified accordingly. Firstly, the cooperative nature of reptation motions in this limit can be accounted for by replacing the number of Kuhn segments per chain, N_{chain}, by $N_{\text{chain}}\sqrt{2\pi d_{\text{pore}}/p}$ [see Eq. (42) below].

Secondly, Eq. (35) must be further supplemented by taking into account the contribution of rotational diffusion modes to the spin-lattice relaxation rate. This should be done because the pore diameter of Vycor is only about 4 nm, so

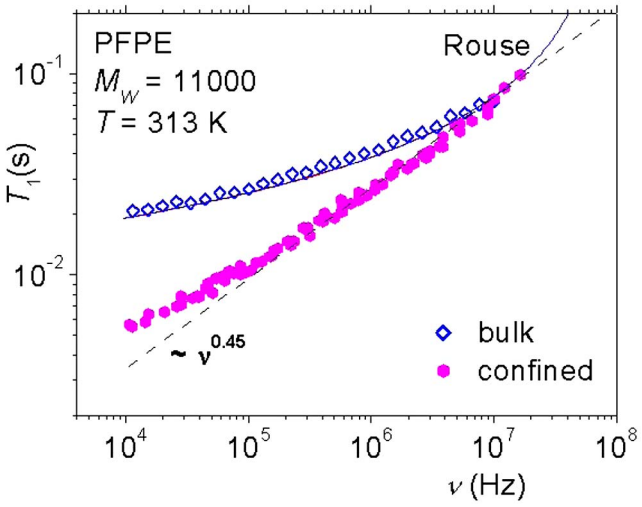

FIG. 2. Fluorine spin-lattice relaxation dispersion curves in bulk PFPE and when confined in silanized Vycor porous glass. The solid line fitting the bulk data represents the Rouse model according to Eq. (33) with the segment fluctuation time $\tau_s = 2\times10^{-9}$ s, $\tilde{M}_2 = 2.7\times10^{-9}$ s^{-2}, and $\tilde{M}_2^* = 2.0\times10^{-9}$ s^{-2}. The data for the confined polymer can be described by a power law $T_1 \propto \nu^{0.45}$ above 10^5 Hz which approaches limit III of the reptation model [see Eq. (36)].

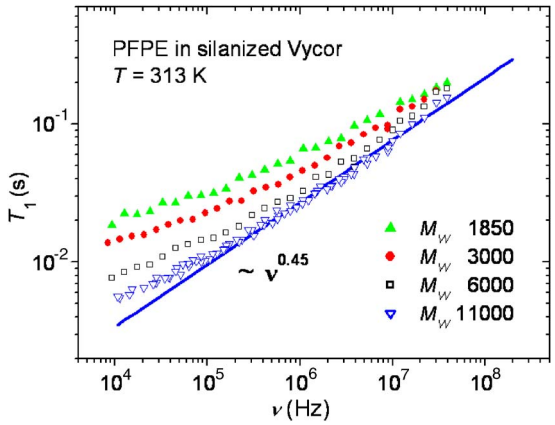

FIG. 3. Frequency dependence of the fluorine spin-lattice relaxation time of PFPE confined in silanized Vycor glass. The curve parameter is the weight-average molecular weight. The slope of the straight line approaches the frequency dependence signature corresponding to region III of the reptation model, $T_1^{\mathrm{rep,III}} \propto \nu^{1/2}$.

that a contribution on this basis is expected for times $t \geqslant t_{\mathrm{expt}} \sim 10^{-7}$ s [see Eq. (19)]. Due to rotational diffusion, the polymer ensemble in the pore moves around the central line. If a polymer chain is displaced a root-mean-square curvilinear distance $\langle s^2(t)\rangle^{1/2}$ along its own contour, the mean displacement along the pore will be $\langle s^2(t)\rangle^{1/2} b/d_{\mathrm{pore}}$. The probability that a polymer segment is still in the initial region of the pore after a time t will be larger by a factor of d_{pore}/b relative to the probability that a polymer segment is still in the initial part of the tight tube.

In Eq. (35), both modifications can roughly be taken into account by multiplying the right-hand side by $(2\pi d_{\mathrm{pore}}/p)^{1/4}$ because of the cooperative character of reptation and by d_{pore}/b due to collective rotational diffusion. The spin-lattice relaxation rate for limit III thus becomes

$$\frac{1}{T_1^{\mathrm{rep,III}}} \approx \frac{32\pi^{1/2}3^{1/2}}{1215}\Gamma(1/2)\cos(\pi/4)(1+2^{3/2}) \times N_{\mathrm{chain}}^{1/2}\frac{b^3\tilde{l}}{d_{\mathrm{pore}}^4}\frac{\tilde{M}_2\tau_s}{(\omega\tau_s)^{1/2}}\left(\frac{2\pi d_{\mathrm{pore}}}{p}\right)^{1/4}\frac{d_{\mathrm{pore}}}{b}. \quad (36)$$

Combining Eqs. (33) and (36), we find for the diameter of the effective tube constraining the cooperative motions of polymer chains

$$d_{\mathrm{eff}} \approx 0.67b\left(\frac{T_1^{\mathrm{rep}}(\omega)}{T^{\mathrm{Rouse}}(\omega)}\frac{\tilde{p}(d_{\mathrm{pore}}/b)\sqrt{N_{\mathrm{chain}}\sqrt{2\pi d_{\mathrm{pore}}/p}}}{(\omega\tau_s)^{1/2}\ln(0.95/\omega\tau_s)}\right)^{1/3}. \quad (37)$$

IV. EXPERIMENTAL RESULTS

Figure 2 demonstrates that there is a strong confinement effect in the spin-lattice relaxation dispersion of PFPE melts when filled into Vycor porous glasses relative to the bulk behavior. The effect evolves relatively slowly parallel to the filling degree of the pores, but saturated conditions are reached after about 10 days.[11] At the lowest frequencies, a plateau of the spin-lattice relaxation dispersion is approached indicating the cutoff by the molecular weight dependent terminal chain mode relaxation time. Above about 10^5 Hz, the dispersion curves represent the chain mode regime of interest in this study.

The experimental conditions were selected so that rotational diffusion modes dominate allowing for correlated reptation characteristics to be visible in the experimental window of spin- lattice relaxation dispersion. The Flory radius of the PFPE melts is about 10 nm and the polymer was confined in 4 nm Vycor porous glass.

The fluorine spin-lattice dispersion curves of the PFPE melts filled into the silanized Vycor reveal strong signatures of the cooperative reptation picture outlined above. This, in particular, refers to the predicted frequency (Fig. 3) and molecular weight dependences (Fig. 4) commonly represented

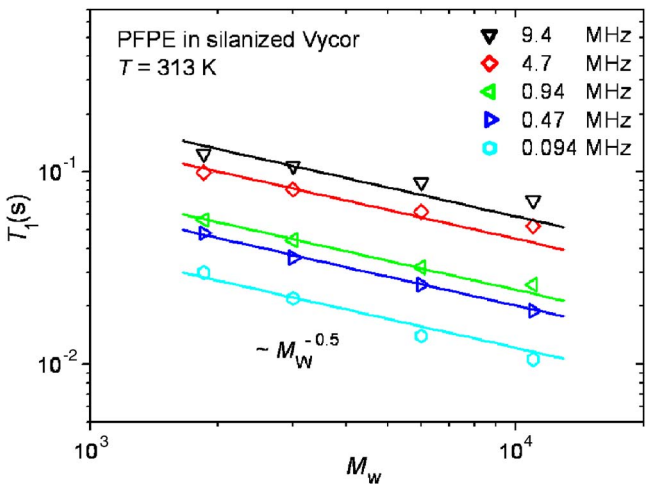

FIG. 4. Molecular weight dependence of the fluorine spin-lattice relaxation time of PFPE confined in silanized Vycor. The curve parameter is the frequency. The straight lines reflect the molecular weight dependence signature corresponding to region III of the reptation model, $T_1^{\mathrm{rep,III}} \propto M^{-1/2}$.

by $T_1^{\text{rep,III}} \propto M_w^{-1/2} \nu^{1/2}$. It appears that limit III of the Doi/Edwards reptation model[7] applies although thermodynamic considerations contradict the predictions of this limiting case. The conclusion is that the formalism modified for cooperative chain dynamics [see Eq. (36)] is verified accordingly.

On the other hand, the bulk PFPE melt satisfactorily reproduces the prediction by the Rouse model in the Larmor frequency range $\tau_R^{-1} \ll \omega \ll \tau_s^{-1}$ [see Eq. (33) and Fig. 2]. The experimental spin-lattice relaxation data for polymer melts in bulk and under confinement permit the estimation of the diameter of the tube effective for cooperative chain dynamics according to Eq. (37). At 10^5 Hz, the spin-lattice relaxation times in bulk and under confinement have been found to be 2.5×10^{-2} s$\hat{=}T_1^{\text{Rouse}}$ and 5×10^{-3} s$\hat{=}T_1^{\text{rep,III}}$, respectively (see Fig. 2). For PFPE with molecular weight of 11 000, we may assume $N_{\text{chain}} \approx 100$, $b \approx 0.6$ nm, $\tilde{p}=1$, and $p \approx 0.2$ nm. Inserting these data into Eq. (37) gives $d_{\text{eff}} \approx 2$ nm. That is, the effective tube diameter has the same order of magnitude as the confinement length scale $d_{\text{pore}} \approx 4$ nm. In the light of the complexity of the pore space geometry in Vycor, this approximate reproduction of the Vycor pore dimension by our model formalism appears to be remarkably close. Thus from the experimental values of the spin-lattice relaxation times, taking cooperative motions of the chains into consideration, we have been able to fit the effective tube diameter to be equal to the actual pore diameter.

V. DISCUSSION

Field-cycling NMR relaxometry in polymer melts confined in nanoscopic pores reveals the signatures predicted for limit III ($t \gg \tau_R$) of the tube/reptation model with respect to both the frequency and molecular weight dependences, $T_1 \propto M^{-1/2} \nu^{1/2}$. On the other hand, general thermodynamic relations allow ordinary reptation only for times shorter than the Rouse relaxation time, while on a much longer time scale no such process can take place. In the present study, we have shown that this contradiction is an apparent one.

The explanation is that chain dynamics under nanoscopic confinements becomes cooperative. The theory of chain dynamics in polymer melts has been revisited for the special conditions valid in nanoscopic pores. The crucial point is that the limitation of fluctuations of the segment number in a given volume is determined by Eq. (24). The ordinary tube/reptation model predicts much larger fluctuations in its limit III. The conclusion is that reptating polymer chains do not move independently of each other but in a correlated manner. Excessive fluctuations of the segment number are avoided in this way while the signatures of limit III predicted for the tube/reptation model still determine the experimental relaxation features. In this respect, it is inessential for limit III whether the reptation displacements of polymer chains occur cooperatively or not.

The cooperativity phenomenon under confinement can also be concluded based on another argument, namely, a random-walk formalism. The curvilinear mean-squared displacement was shown to be reduced relative to the reptation prediction given in Eq. (31). There are n_t different tubes in the considered pore space volume. Let the tubes be numbered by the subscript $i=1,\ldots,n_t$. The number of segments in these tubes varies in the time t by an amount $n_{si}(t)$, which can be positive or negative. The total number of segments thus changes in time t by

$$m(t) = \sum_{i=1,\ldots,n_t} n_{si}(t). \tag{38}$$

For simplicity, we assume that all numbers $n_{si}(t)$ have the same absolute magnitude $|n_s(t)|$ but can have different signs. Then, ordinary reptation is equivalent to a one-dimensional discrete random walk:[18] The random walker performs n_t random jumps of length $|n_s(t)|$. The total displacement to the right is then

$$m(t) = k|n(t)|, \tag{39}$$

where $k=l-n_t/2$ and l is the number of jumps to the right. The probability for this displacement is[18]

$$P(m(t)) = \frac{1}{\sqrt{2\pi n_t}} \exp\left\{-\frac{k^2}{2n_t}\right\}. \tag{40}$$

In the present situation, $m(t)$ is the total change of polymer segments in a given volume V due to reptation of polymer chains in their own tubes. In the short-time limit, $t \ll \tau_R$, all values of $m(t)$ are possible. In the opposite limit, $t \gg \tau_R$, even the number $|n(t)|$ becomes too large to be compatible with the thermodynamically allowed total change of the number of polymer segments in a volume V. We therefore set $k=0$ so that

$$P(m(t)=0) = \frac{1}{\sqrt{2\pi n_t}}. \tag{41}$$

As a consequence, Eq. (31) must be modified according to

$$\langle s^2(t) \rangle \simeq \frac{2}{3\pi^2} b^2 \frac{t}{N_{\text{chain}} \tau_s} \frac{1}{\sqrt{2\pi n_t}} = \frac{2}{3\pi^2} b^2 \frac{t}{N_{\text{chain}} \tau_s} \sqrt{\frac{p}{2\pi d_{\text{pore}}}}. \tag{42}$$

This is the simplest semiphenomenological way of taking into account the strong cooperative character of chain reptations in polymer melts confined in cylindrical pores of diameter d_{pore}. The molecular mass dependence is obviously the same as in the ordinary reptation model, whereas the mean-squared curvilinear displacement is reduced by a factor of $\sqrt{p/2\pi d_{\text{pore}}}$. The latter effect is a consequence of the strongly cooperative nature of chain motions in the volume V.

An important consequence of the above results is that chain modes in bulk polymer melts should also be strongly cooperative in the limit $t \gg \tau_R$. The same sort of argument as in the present treatment applies in this case with only minor modifications. Corresponding work is in progress.

ACKNOWLEDGMENTS

The authors thank Professor N. Hüsing for the silanized Vycor samples and Hans Wiringer for assistance in the

course of the experiments. This work was supported by the Volkswagen-Stiftung, the Deutsche Forschungsgemeinschaft, and RFBR.

[1] C. Mattea, N. Fatkullin, E. Fischer, U. Beginn, E. Anoardo, M. Kroutieva, and R. Kimmich, Appl. Magn. Reson. **27**, 371 (2004).
[2] N. Fatkullin, R. Kimmich, E. Fischer, C. Mattea, U. Beginn, and M. Kroutieva, New J. Phys. **6**, 46 (2004) (http://www.njp.org/).
[3] R. Kimmich, R.-O. Seitter, U. Beginn, M. Möller, and N. Fatkullin, Chem. Phys. Lett. **307**, 147 (1999).
[4] R. Kausik, C. Mattea, N. Fatkullin, and R. Kimmich, J. Chem. Phys. **124**, 114903 (2006).
[5] R. Kimmich and E. Anoardo, Prog. Nucl. Magn. Reson. Spectrosc. **44**, 257 (2004).
[6] M. Doi and S. F. Edwards, *The Theory of Polymer Dynamics* (Clarendon, Oxford, 1986).
[7] R. Kimmich and N. Fatkullin, Adv. Polym. Sci. **170**, 1 (2004).
[8] S. Kariyo and S. Stapf, Macromol. Chem. Phys. **206**, 1300 (2005).
[9] S. Kariyo, C. Gainaru, H. Schick, A. Brodin, V. N. Novikov, and E. A. Rössler, Phys. Rev. Lett. **97**, 207803 (2006).
[10] N. Fatkullin and R. Kimmich, Macromol. Symp. **237**, 69 (2006).
[11] R. Kausik, C. Mattea, R. Kimmich, and N. Fatkullin, Eur. Phys. J., Special Topics (to be published).
[12] R. Kausik, N. Fatkullin, N. Hüsing, and R. Kimmich, Magn. Reson. Imaging (to be published).
[13] A. M. Kosevich, E. M. Lifshitz, L. D. Landau, and L. P. Pitaevskii, *Theory of Elasticity* (Butterworth-Heinemann, Oxford, 1986).
[14] R. Balesku, *Equilibrium and Nonequilibrium Statistical Mechanics* (Wiley, New York, 1975).
[15] A. Denissov, M. Kroutieva, N. Fatkullin, and R. Kimmich, J. Chem. Phys. **116**, 5217 (2002).
[16] R. Ullman, J. Chem. Phys. **43**, 3161 (1965).
[17] T. N. Khazanovich, Polym. Sci. U.S.S.R. **4**, 727 (1963).
[18] S. Chandrasehkar, Rev. Mod. Phys. **15**, 1 (1943).